11-30-2011

Nondestructive Electrothermal Detection of Corrosion

Brittany Ambeau
Rose-Hulman Institute of Technology

Harris Enniss
Rose-Hulman Institute of Technology

Stefan Schnake
Rose-Hulman Institute of Technology

Nondestructive Electrothermal Detection of Corrosion

B. Ambeau, H. Enniss, and S. Schnake

Adviser: Kurt M. Bryan

Mathematical Sciences Technical Report Series
MSTR 11-04

November 30, 2011

Department of Mathematics
Rose-Hulman Institute of Technology
http://www.rose-hulman.edu/math

Fax (812)-877-8333 **Phone (812)-877-8193**

Nondestructive Electrothermal Detection of Corrosion

Brittany Ambeau, Harris Enniss, and Stefan Schnake

November 30, 2011

Abstract

Nondestructive testing and imaging plays an important role in many industries, e.g., the monitoring and maintenance of corrosion in aircraft. The general technique is to input energy in some form into an object, observe the object's response, and from this input-output information determine the internal structure.

New techniques are always being explored, and recently there has been much interest in methods that use multiple forms of energy. In this vein, we examine a new technique for imaging corrosion or material loss in an object by combining electrical and thermal measurements on some accessible portion of the object's outer boundary. The flow of electrical and thermal energy through the object is modeled using partial differential equations, and imaging the corrosion leads to a mathematical "inverse problem." We examine limits and stability of this type of imaging, and develop an effective numerical algorithm for solving these types of problems.

Contents

Chapter 1

Introduction

1.1 Context and motivation

In many structural contexts, it is important to be able to inspect the interior of some object for defects or voids. A number of methods have been tested or implemented to allow such inspection without requiring disassembly or destruction of the object in question. One promising method is electrothermal imaging, whereby an electric current generates heat within an object, and the resulting temperature distribution can be used to obtain an image of the object.

In the problem examined here, we assume a nearly-rectangular, homogeneously electric and thermal conducting domain Ω of length L and height 1 of which one boundary, Γ, is damaged. We assume Γ can be parameterized as the graph of a continuously differentiable function $S(x)$, where S has support strictly contained in the interval $(0, L)$. On the sides of the rectangle ($\{x = 0, 0 \leq y \leq 1\}$ and $\{x = L, 0 \leq y \leq 1\}$) we input a nonzero electric current. Figure 1.1 shows the physical setting of the problem. Electrical current flows from left to right through Ω

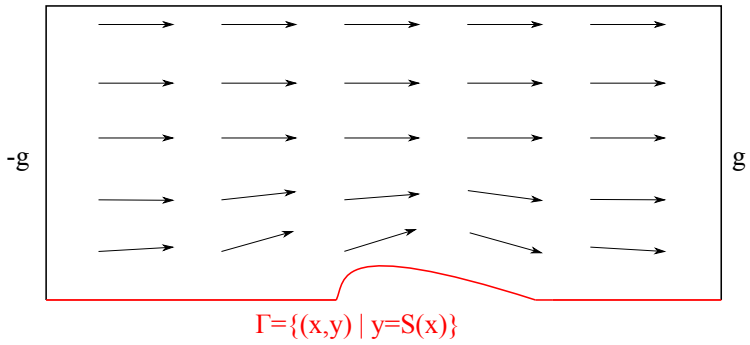

Figure 1.1: Physical Setting

around the void delineated by $S(x)$. In the narrowest regions of Ω, above the peaks of $S(x)$, the current flow is increased by the void, and so the voltage drops more rapidly. At the same time, this increase in current means an increase in resistive heating. Hot-spots appear where current is strongest, and heat propagates outwards to the surface where it can be observed.

In practice, both voltage and temperature can be observed, and either can be used to produce an image of the damage profile $S(x)$. Such measurements might be used to obtain an image of a structural member where it adjoins some other component, or, with modifications to the domain and boundary conditions, the interior of a pipe, or in other contexts where it is difficult or impossible to access the face of some object.

We should note that other input current fluxes could be used, but most of our reconstructions focus on this particular input flux for simplicity.

1.2 Contents

The report is organized as follows. In Chapter 2 we examine the purely electrical version of the problem. We (1) give a detailed statement of the inverse problem, (2) form a linearized version of such inverse problem, that is, we linearize a relationship between the back surface described by $S(x)$ and the voltage data, (3) construct and regularize an algorithm for recovering estimates of the back surface, and (4) provide a number of examples. In Chapter 3 we examine the electrothermal version of the problem. In this version we use temperature data to obtain a solution. Discussion of our results and conclusive remarks are included in Chapter 4.

Chapter 2

Electrical Case

If we inject an electrical current flux g (constant flux per unit length) on the left boundary and remove a constant current flux g on the right boundary, as in Figure 1.1, and assume for convenience that the region Ω has a constant electrical conductivity of 1, then the standard model for conduction shows that the electric potential $u = u(x, y)$ inside Ω satisfies

$$\begin{aligned}
\Delta u &= 0 \text{ in } \Omega && (2.1)\\
\frac{\partial u}{\partial \mathbf{n}} &= 0 \text{ on } \Gamma && (2.2)\\
\frac{\partial u}{\partial \mathbf{n}} &= 0 \text{ on } \partial\Omega \cap \{y = 1\} && (2.3)\\
\frac{\partial u}{\partial \mathbf{n}} &= g \text{ on } \partial\Omega \cap \{x = 0\} && (2.4)\\
\frac{\partial u}{\partial \mathbf{n}} &= -g \text{ on } \partial\Omega \cap \{x = 1\} && (2.5)
\end{aligned}$$

where Γ denotes the potentially damaged back surface. Here we are assuming that the damaged surface is electrically insulating. Note that (2.1)-(2.5) determines u only up to an arbitrary additive constant; the value of this constant does not matter, but can be uniquely determined with an additional normalization, e.g., $\int_{\partial\Omega} u\, ds = 0$.

The inverse problem we are interested in is this: We input a flux g and measure u on the top surface, and from this information we want to deduce the function $S(x)$.

2.1 Linearization

Given knowledge of the domain, and in particular the function $S(x)$, we can in principle compute u in Ω. Thus there is some "back surface to data" map $M : C^1(\Gamma) \to C^0(\text{top})$ defined by $M(S) = u(x, 1)$ where u satisfies (2.1)-(2.5). We would like to find an inverse map M^{-1} that allows us to compute $S(x)$ from knowledge of $u(x, 1)$.

The mapping M is nonlinear, however, and the problem is greatly simplified if we linearize M about the "nominal" uncorroded back surface $y = 0$. This is also physically reasonable, since we expect corrosion to be relatively small. To this end, let us suppose that S is of the form $S(x) = \epsilon S_0(x)$ for some function S_0 and "small" $\epsilon > 0$. We seek an approximation solution $u = u_0 + \epsilon\hat{u}$ to (2.1)-(2.5), with error of order $O(\epsilon^2)$, where u_0 is the solution to (2.1)-(2.5) with

undamaged back surface $S \equiv 0$. Specifically, u_0 satisfies

$$\begin{aligned}
\Delta u_0 &= 0 \text{ in } \Omega_0 && (2.6)\\
\frac{\partial u_0}{\partial \mathbf{n}} &= 0 \text{ on } \partial\Omega_0 \cap \{y = 0\} && (2.7)\\
\frac{\partial u_0}{\partial \mathbf{n}} &= 0 \text{ on } \partial\Omega_0 \cap \{y = 1\} && (2.8)\\
\frac{\partial u_0}{\partial \mathbf{n}} &= g \text{ on } \partial\Omega_0 \cap \{x = 0\} && (2.9)\\
\frac{\partial u_0}{\partial \mathbf{n}} &= -g \text{ on } \partial\Omega_0 \cap \{x = 1\} && (2.10)
\end{aligned}$$

on the rectangle $\Omega_0 = (0, L) \times (0, 1)$. The function u_0 can be computed, and in fact for this simple input flux $u_0(x, y) = -gx$ (up to an additive constant).

For simplicity we define $\epsilon\hat{u} = \bar{u}$. Following [NS], the function $\bar{u}$ must (formally) satisfy

$$\begin{aligned}
\Delta \bar{u} &= 0 \text{ in } \Omega && (2.11)\\
\frac{\partial \bar{u}}{\partial \mathbf{n}} &= -\frac{\partial}{\partial x}\left(S(x)\frac{\partial u_0}{\partial x}(x, 0)\right) \text{ on } \Gamma && (2.12)\\
\frac{\partial \bar{u}}{\partial \mathbf{n}} &= 0 \text{ on } \partial\Omega \setminus \Gamma && (2.13)
\end{aligned}$$

obtained by plugging $u = u_0 + \epsilon\hat{u}$ into equations (2.1)-(2.5), expanding into power series in ϵ about $\epsilon = 0$, and dropping terms of order ϵ^2 and higher.

In what follows we replace equations (2.1)-(2.5) governing the nonlinear forward problem with their linearized versions (2.11)-(2.13). Note that the function $\bar{u}$ is also determined only up to an arbitrary additive constant.

2.2 Solving the Forward and Inverse Problem

A standard separation of variables allows us to deduce that any function satisfying the PDE (2.11) and boundary condition (2.13) must be of the form

$$\bar{u}(x, y) = \frac{1}{2}\sum_{k=0}^{\infty} c_k(e^{-\lambda_k + \lambda_k y} + e^{\lambda_k - \lambda_k y})\cos(\lambda_k x) \tag{2.14}$$

for some constants c_k, where $\lambda_k = \frac{k\pi}{L}$. The constants c_k could be determined from $S(x)$, but of course we don't know S. What we do know is $\bar{u}(x, 1)$, the measured voltage data, and this can instead be used to determine the c_k, from which $\bar{u}$ can be found, and then S.

In particular, from (2.14) we have (using $y = 1$)

$$\bar{u}(x, 1) = \sum_{k=0}^{\infty} c_k \cos(\lambda_k x).$$

Since $\bar{u}(x, 1)$ can be expressed via a Fourier series, we know

$$c_k = \frac{2}{L}\int_0^L \bar{u}(x, 1)\cos(\lambda_k x)\, dx \tag{2.15}$$

for all $k \in \mathbb{N}$. Since $\bar{u}(x, 1)$ can be measured along the top surface, we can use (2.15) to recover the c_k for all $k \in \mathbb{N}$ and from that $\bar{u}(x, y)$ on all of Ω.

To recover S itself, note that on Γ (2.12) tells us

$$\frac{\partial \bar{u}}{\partial \mathbf{n}} = -\frac{\partial}{\partial x}\left(S(x)\frac{\partial u_0}{\partial x}(x, 0)\right). \tag{2.16}$$

In addition we can we can take the derivative of (2.14) with respect to the outward normal vector which in this case is the negative derivative with respect to y. This gives us

$$\frac{\partial \bar{u}}{\partial \mathbf{n}} = -\bar{u}_y(x,0) = \frac{1}{2}\sum_{k=0}^{\infty} \lambda_k c_k (e^{-\lambda_k} - e^{\lambda_k}) \cos(\lambda_k x). \tag{2.17}$$

Equating (2.16) and (2.17) forces $S(x)$ to satisfy the differential equation

$$\frac{\partial}{\partial x}\left(S(x)\frac{\partial u_0}{\partial x}(x,0)\right) = \frac{1}{2}\sum_{k=0}^{\infty} \lambda_k c_k (e^{-\lambda_k} - e^{\lambda_k}) \cos(\lambda_k x). \tag{2.18}$$

As noted above, solving (2.6) - (2.10) gives us the solution

$$u_0(x,y) = -gx \tag{2.19}$$

on Ω_0. Substituting (2.19) into (2.18) gives us

$$g\frac{\partial S}{\partial x} = \frac{1}{2}\sum_{k=0}^{\infty} \lambda_k c_k (e^{-\lambda_k} - e^{\lambda_k}) \cos(\lambda_k x) \tag{2.20}$$

which we must solve for $S(x)$. Indeed, if we divide both sides by g and integrate in x (with the assumption $S(0) = 0$, i.e., the corrosion does not extend to the edge of the sample) we obtain

$$S(x) = \sum_{k=1}^{\infty} d_k \sin(\lambda_k x) \tag{2.21}$$

with

$$d_k = \frac{e^{-\lambda_k} - e^{\lambda_k}}{2g} c_k \tag{2.22}$$

a Fourier sine series for S. This allows us to recover $S(x)$ with any nonzero input flux g. In particular, we have shown

Lemma 1. *Let $\bar{u}$ denote the solution to (2.11)-(2.13). The data $\bar{u}(x,1)$ for $0 < x < L$ uniquely determines the function S if $S(0) = 0$.*

2.3 Numerical Approximation

Using COMSOL Multiphysics, we created a damage profile on a rectangle with length 20 and height 1, and simulated an electric current $g = 1$ injected at the left side and pulled from the right. We then took a sampling of the voltage at 401 locations distributed uniformly across the top surface. In order to obtain the coefficients c_k we used a trapezoidal approximation of (2.15). Using Maple 14, we approximated $S(x)$ by truncating the infinite sum in (2.21).

Let N denote the number of terms summed in (2.21). Figure 2.1 is a graph of our approximation with $N = 8$, and with the solid line being our approximation and the dashed line being the actual $S(x)$ where $S(x) = \frac{3}{40}\sqrt{-x^2 + 24x - 128}$ when $x \in [8, 16]$ and 0 otherwise. The approximation was constructed with voltage data that had Gaussian noise level of 0.01. Figure 2.2 shows the next four graphs when $N = 16$, 32, 48, and 64 respectively.

Noise dominates this reconstruction as N grows. This can be seen by noting that noise in the measured data induces noise in the Fourier coefficients, and so we obtain noisy coefficients given by

$$\tilde{c}_k = c_k + E_k \tag{2.23}$$

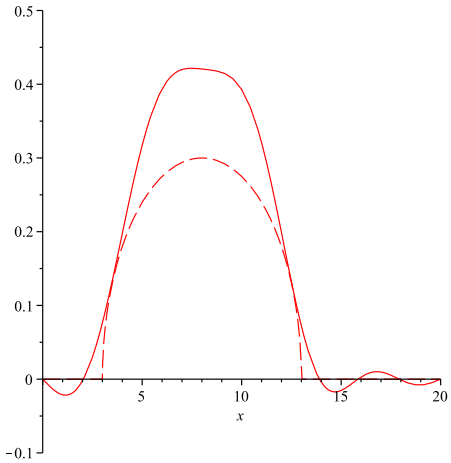

Figure 2.1: Approximation with $N = 8$

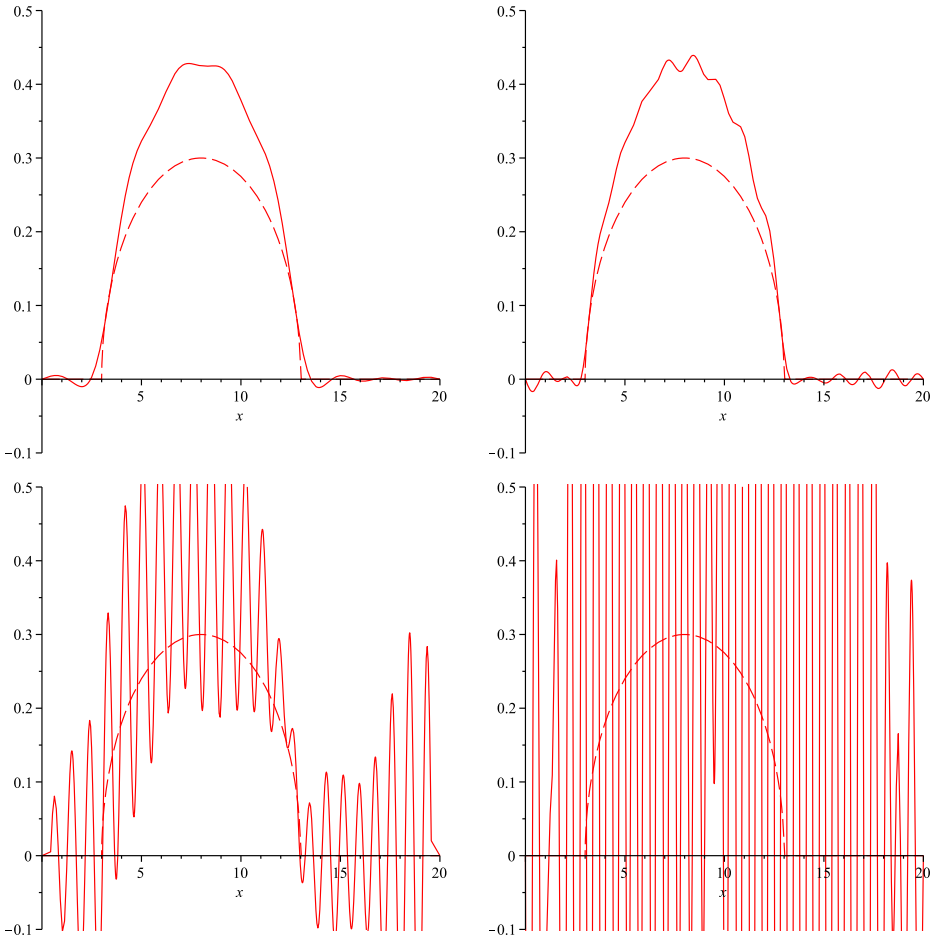

Figure 2.2: Approximation with 16, 32, 48, and 64 terms

for some error sequence E_k. The magnitude of the E_k can be estimated from the amount of noise in the data. Then from (2.20), the measured Fourier coefficients for the boundary condition are given by

$$\tilde{d}_k = d_k = \frac{e^{-\lambda_k} - e^{\lambda_k}}{2g}(c_k + E_k) = d_k + \frac{e^{-\lambda_k} - e^{\lambda_k}}{2g}E_k. \tag{2.24}$$

Any error E_k in approximating c_k will by magnified by this growing exponential. The high-

frequency terms therefore contain substantial noise, and cannot be trusted in the reconstruction.

2.4 Regularization

Truncation of the Fourier expansion allows us to remove high frequency noise, but is a rather crude approach. A more careful method gradually phases out high frequency terms by applying a weight in the range $[0, 1]$ to each coefficient. Let d_k be given by equation (2.22). If we know the c_k exactly then we know the d_k. However, we only know an approximate value for $\tilde{c}_k$ given by equation (2.23), and hence an erroneous value $\tilde{d}_k$ given by equation (2.24). We wish to perform a weighted reconstruction of the form

$$\tilde{S}(x) = \sum_{k=1}^{\infty} w_k \tilde{d}_k \sin(\lambda_k x) \tag{2.25}$$

where the weights w_k gradually decrease from 1 to 0. From (2.21) and (2.25) we have

$$\begin{aligned} S(x) - \tilde{S}(x) &= \sum_{k=1}^{\infty} (d_k - w_k \tilde{d}_k) \sin(\lambda_k x) \\ &= \sum_{k=1}^{\infty} (d_k(1 - w_k) + w_k(e^{-\lambda_k} - e^{\lambda_k})E_k/2g) \sin(\lambda_k x). \end{aligned}$$

Parseval's identity applied to the sine series on the interval $(0, L)$ yields

$$\|S - \tilde{S}\|^2_{L^2(0,L)} = \frac{L}{2} \sum_{k=1}^{\infty} (d_k(1 - w_k) + w_k(e^{-\lambda_k} - e^{\lambda_k})E_k/2g)^2 \tag{2.26}$$

We seek those w_k that minimize the above expression. We can clearly work term by term in k. The value w_k that minimizes $(c_k(1 - w_k) - w_k E_k)^2$ is easily found by differentiating with respect to w_k, to obtain

$$2(d_k(1 - w_k) + w_k(e^{-\lambda_k} - e^{\lambda_k})E_k/2g)(-d_k + (e^{-\lambda_k} - e^{\lambda_k})E_k/2g) = 0.$$

The solution is

$$w_k = \frac{g d_k}{g d_k + E_k(e^{\lambda_k} - e^{-\lambda_k})/2}.$$

Note that if $E_k = 0$ then $w_k = 1$, as expected, while if $E_k \neq 0$ and k is large then $w_k \approx 0$. That the formula for w_k depends on d_k and E_k would seem to be a problem. Ultimately, however, we need not know the precise form, but only the general manner of decay. First, we may estimate or bound the value of E_k, say $|E_k| \leq E$ for some constant E (that depends on the noise level in the data). We then have

$$w_k = \frac{g d_k}{g d_k + E(e^{\lambda_k} - e^{-\lambda_k})/2}.$$

Also, we may make reasonable assumptions about the manner in which the Fourier coefficients d_k decay to zero, e.g.,

$$d_k \approx \frac{1}{C(k+1)^2}.$$

Other forms could be considered, but this typical for twice continuously differentiable functions S. Tests with typical sample damage profiles suggest $C = 196$ as a reasonable coefficient. This yields a regularized solution which may be more useful, as below, in which we use $E = 10^{-5}$.

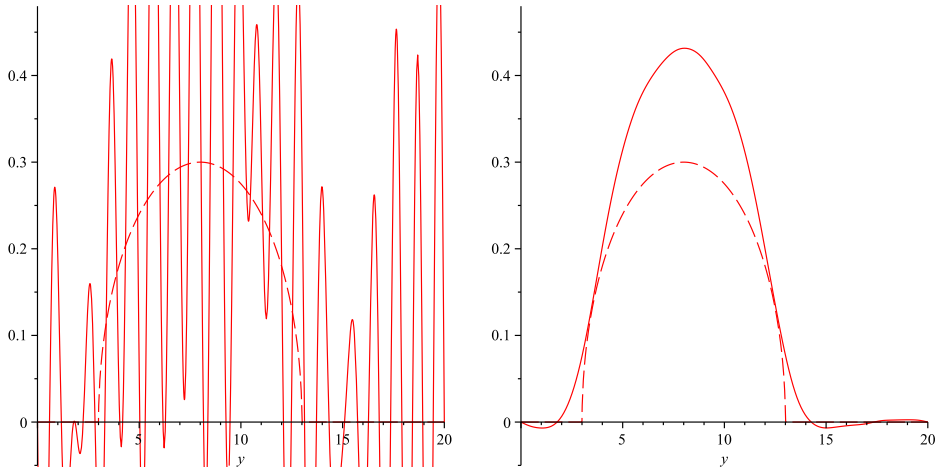

2.5 Summary

By linearizing the mapping between damage profiles and voltage, we can produce an approximate PDE from which we can reproduce the profile of a damaged surface. This method suffers from excessive noise, and must be regularized to produce useful data.

Chapter 3

Electrothermal Case

When electrical current flows through an object with any resistance, heat is generated. Let $v(x, y, t)$ denote the temperature of Ω at any given time. Our goal in this chapter is to explore the possibility of using measurements of v on the accessible portion of Ω to determine the corrosion profile on the back surface.

By Joule's Law, the rate of heat production per area of Ω per unit time is assumed to be in proportion to the square of the current magnitude. We assume that after suitable rescaling the function v satisfies

$$\frac{\partial v}{\partial t} - \Delta v = |\nabla u|^2 \text{ in } \Omega \times [0, \infty). \tag{3.1}$$

If we assume our experiment starts at $t = 0$, with zero initial temperature, then we have the initial condition $v(x, y, 0) = 0$ in Ω. We also need boundary conditions for v. For simplicity, we consider the case where the domain is thermally insulated, so $\frac{\partial v}{\partial \mathbf{n}} = 0$ at all points on $\partial\Omega$.

In general, the electrothermal problem is described by equations (2.6) – (2.10) and (3.1), along with

$$\frac{\partial v}{\partial \mathbf{n}} = 0 \text{ on } \Gamma \tag{3.2}$$

$$\frac{\partial v}{\partial \mathbf{n}} = 0 \text{ on } \partial\Omega \setminus \Gamma \tag{3.3}$$

$$v(x, y, 0) = 0 \text{ for all } x, y \text{ in } [0, L] \times [0, 1]. \tag{3.4}$$

3.1 Linearization

We intend to use the data $v(x, 1, t)$ to recover S. However, similar to the Electric Case, the mapping $S(x) \to v(x, 1, t)$ is nonlinear, therefore, we shall (formally) linearize. We want to find a $\hat{v}$ such that $v_0 + \varepsilon\hat{v} = v_0 + \bar{v}$ approximately satisfies the PDE for $S(x) = \varepsilon S_0(x)$, where v_0 is the temperature on an undamaged rectangle. Thus,

$$\frac{\partial(v_0 + \varepsilon\hat{v})}{\partial t} - \Delta(v_0 + \varepsilon\hat{v}) = |\nabla(u_0 + \varepsilon\hat{u})|^2 \text{ in } \Omega \times [0, \infty) \tag{3.5}$$

$$\frac{\partial(v_0 + \varepsilon\hat{v})}{\partial \mathbf{n}} = 0 \text{ on } \Gamma \tag{3.6}$$

$$\frac{\partial(v_0 + \varepsilon\hat{v})}{\partial \mathbf{n}} = 0 \text{ on } \partial\Omega \setminus \Gamma \tag{3.7}$$

$$v_0(x, y, 0) + \varepsilon\hat{v}(x, y, 0) = 0 \text{ for all } x, y \text{ in } [0, L] \times [0, 1] \tag{3.8}$$

Using the initial PDE, equations (3.5) through (3.8) become

$$\begin{aligned}
\frac{\partial \hat{v}}{\partial t} - \Delta \hat{v} &= \frac{|\nabla(u_0 + \varepsilon\hat{u})|^2 - |\nabla u_0|^2}{\varepsilon} \text{ in } \Omega \times [0,\infty) && (3.9)\\
\frac{\partial \hat{v}}{\partial \mathbf{n}} &= 0 \text{ on } \Gamma && (3.10)\\
\frac{\partial \hat{v}}{\partial \mathbf{n}} &= -\frac{1}{\varepsilon}\frac{\partial v_0}{\partial \mathbf{n}} \text{ on } \partial\Omega \setminus \Gamma && (3.11)\\
\hat{v}(x,y,0) &= 0 \text{ for all } x, y \text{ in } [0,L] \times [0,1] && (3.12)
\end{aligned}$$

Simplifying (3.9) we obtain

$$\begin{aligned}
\frac{\partial \hat{v}}{\partial t} - \Delta \hat{v} &= \frac{|\nabla(u_0 + \varepsilon\hat{u})|^2 - |\nabla u_0|^2}{\varepsilon}\\
&= \frac{\nabla(u_0 + \varepsilon\hat{u}) \cdot \nabla(u_0 + \varepsilon\hat{u}) - \nabla(u_0) \cdot \nabla(u_0)}{\varepsilon}\\
&= 2(\nabla u_0 \cdot \nabla \hat{u}) + \varepsilon|\nabla \hat{u}|^2.
\end{aligned}$$

Because $\varepsilon|\nabla\hat{u}|^2$ should be close to zero when ϵ is near zero, we have justification to drop this term and write

$$\frac{\partial \hat{v}}{\partial t} - \Delta \hat{v} = 2(\nabla u_0 \cdot \nabla \hat{u}) \text{ in } \Omega \times [0,\infty) \tag{3.13}$$

or

$$\frac{\partial \bar{v}}{\partial t} - \Delta \bar{v} = 2(\nabla u_0 \cdot \nabla \bar{u}) \text{ in } \Omega \times [0,\infty). \tag{3.14}$$

3.2 Techniques for Solution

Again, similar to the Electrical Case, we will focus on the case in which we inject current at one side and pull it out at the other. Using boundary conditions (2.2) - (2.5), we obtain $u_0 = -gx$. This forces $\nabla u_0 \cdot \nabla \bar{u} = \frac{\partial \bar{u}}{\partial x}$. By solving for v_0 in (3.2) - (3.4), we have $v_0 = t$ for all $(x, y) \in [0, L] \times [0, 1]$. These substitutions change (3.9) through (3.12) into

$$\begin{aligned}
\frac{\partial \bar{v}}{\partial t} - \Delta \bar{v} &= 2\frac{\partial \bar{u}}{\partial x} \text{ in } \Omega \times [0,\infty) && (3.15)\\
\frac{\partial \bar{v}}{\partial \mathbf{n}} &= 0 \text{ on } \partial\Omega && (3.16)\\
\bar{v}(x,y,0) &= 0. && (3.17)
\end{aligned}$$

Proceeding as suggested by [KB], let $S(x)$ be given the by following Fourier sine expansion

$$S(x) = \sum_{k=1}^{\infty} S_k \sin(\lambda_k x) \tag{3.18}$$

where $\lambda_k = \frac{k\pi}{L}$. Note that the derivative of $S(x)$ is

$$\frac{\partial S}{\partial x} = \sum_{k=1}^{\infty} \lambda_k S_k \cos(\lambda_k x). \tag{3.19}$$

However we also have a form for the derivative of $S(x)$ given by (2.20). Comparing (2.20) and (3.19) shows us

$$\frac{1}{2}c_k = \frac{S_k}{e^{-\lambda_k} - e^{\lambda_k}}$$

for all $k \in \mathbb{N}$. By doing this we can compute $S(x)$ only up to an additive constant. We can modify $\bar{u}(x,y)$ to be

$$\bar{u}(x,y) = \sum_{k=1}^{\infty} \frac{S_k}{e^{-\lambda_k} - e^{\lambda_k}} (e^{-\lambda_k + \lambda_k y} + e^{\lambda_k - \lambda_k y}) \cos(\lambda_k x). \tag{3.20}$$

With some minor computations, we obtain

$$2\frac{\partial \bar{u}}{\partial x}(x,y) = -\sum_{k=1}^{\infty} \frac{2\lambda_k S_k}{e^{-\lambda_k} - e^{\lambda_k}} (e^{-\lambda_k + \lambda_k y} + e^{\lambda_k - \lambda_k y}) \sin(\lambda_k x). \tag{3.21}$$

A standard separation of variables shows that

Lemma 2. *In general, $\bar{v}$ will have the form*

$$\bar{v}(x,y,t) = \sum_{j,m=0} \phi_{jm}(t) \cos(\lambda_j x) \cos(m\pi y)$$

for some sequence of functions $\phi_{jm}(t)$.

Indeed, we can compute the ϕ_{jm}. Substituting $\bar{v}(x,y,t)$ into (3.15) gives us

$$\bar{v}_t - \Delta \bar{v} = \sum_{j,m=0} (\phi'_{jm}(t) + \mu_{jm}\phi_{jm}(t)) \cos(\lambda_j x) \cos(m\pi y) \tag{3.22}$$

where $\mu_{jm} = \pi^2(j^2/L^2 + m^2)$. Let $2\frac{\partial \bar{u}}{\partial x}(x,y)$ have the following Fourier cosine-cosine expansion.

$$2\frac{\partial \bar{u}}{\partial x}(x,y) = \sum_{j=0,m=0}^{\infty} a_{jm} \cos(\lambda_j x) \cos(m\pi y) \tag{3.23}$$

where the constants a_{jm} are given by

$$a_{jm} = \frac{q_{jm}}{L} \int_0^L \int_0^1 2\frac{\partial \bar{u}}{\partial x}(x,y) \cos(\lambda_j x) \cos(m\pi y)\, dy\, dx \tag{3.24}$$

where $q_{jm} = 4$ if $j, m > 0$, $q_{jm} = 2$ if $j = 0$ or $m = 0$ (but not both), and $q_{00} = 1$. Comparing the coefficients in (3.22) and (3.23) shows that $\phi_{jm}(t)$ must satisfy the following ODE

$$\phi'_{jm}(t) + \mu_{jm}\phi_{jm}(t) = a_{jm}. \tag{3.25}$$

Solving (3.25) for $\phi_{jm}(t)$ gives

$$\phi_{jm}(t) = \frac{a_{jm}}{\mu_{jm}}(1 - e^{-\mu_{jm}t}) \tag{3.26}$$

for $(j,m) \neq (0,0)$ and $\phi_{00}(t) = a_{00}t$. Substituting $\phi_{jm}(t)$ into (3.22) gives us

$$\bar{v}(x,y,t) = a_{00}t + \sum_{\substack{j\neq 0 \\ m\neq 0}} \frac{a_{jm}}{\mu_{jm}}(1 - e^{-\mu_{jm}t}) \cos(\lambda_j x) \cos(m\pi y) \tag{3.27}$$

In order to compute a_{jm} we can use (3.24) and (3.21) to obtain

$$\begin{aligned} a_{jm} &= -\frac{q_{jm}}{L} \int_0^L \int_0^1 \sum_{k=1}^{\infty} \frac{2\lambda_k S_k (e^{-\lambda_k + \lambda_k y} + e^{\lambda_k - \lambda_k y})}{e^{-\lambda_k} - e^{\lambda_k}} \sin(\lambda_k x) \\ &\quad \times \cos(\lambda_j x) \cos(m\pi y)\, dy\, dx \end{aligned} \tag{3.28}$$

The integrals can by evaluated using the following properties:

$$\int_0^L \cos(\lambda_j x)\sin(\lambda_k x)\,dx = -\frac{Lk(1+(-1)^{j+k+1})}{\pi(j^2-k^2)} \tag{3.29}$$

$$\int_0^1 \cos(m\pi y)(e^{-\lambda_k+\lambda_k y}+e^{\lambda_k-\lambda_k y})\,dy = -\frac{Lk(e^{-\lambda_k}-e^{\lambda_k})}{\pi(k^2+m^2L^2)}. \tag{3.30}$$

Using (3.29) and (3.30) to solve the left side of (3.28) gives us a form for a_{jm}

$$a_{jm} = q_{jm}\sum_{\substack{k=1\\k\neq j}}^{\infty}\frac{2k^3S_k(1+(-1)^{j+k+1})}{\pi(j^2-k^2)(k^2+m^2L^2)} \tag{3.31}$$

for $j \neq 0$ and $m \neq 0$, while

$$a_{00} = -\sum_{k=1}^{\infty}\frac{2S_k(1+(-1)^{k+1})}{\pi k}. \tag{3.32}$$

It is important to see that while $j \neq k$ when adding across k in (3.31), if $j = k$, then (3.29) shows us that the term would be 0. Therefore we are not affecting $a_{j,m}$ by removing this special case.

Lemma 2 along with equations (3.26), (3.31) and (3.32) give the function $\bar{v}$ in terms of the Fourier coefficients S_k of the function S.

3.3 The Inverse Problem

We now show how to use these computations to solve the inverse problem of recovering S from the top surface data $v(x,1,t)$ where $0 < x < L$ and t ranges over some interval $0 < t < T$. Since we are measuring the heat across the top surface on some time interval, we know

$$\bar{v}(x,1,t) = a_{00}t + \sum_{\substack{j\neq 0\\m\neq 0}}(-1)^m\frac{a_{jm}}{\mu_{jm}}(1-e^{-\mu_{jm}t})\cos(j\pi x/L). \tag{3.33}$$

We can also suppose $\bar{v}(x,1,t)$ has the Fourier cosine expansion

$$\bar{v}(x,1,t) = \sum_{n=0}^{\infty} f_n(t)\cos(\lambda_n x) \tag{3.34}$$

where

$$f_n(t) = \frac{2}{L}\int_0^L \bar{v}(x,1,t)\cos(\lambda_n x)\,dx$$

for all $n \in \mathbb{N}$ and

$$f_0(t) = \frac{1}{L}\int_0^L \bar{v}(x,1,t)\,dx$$

when $n = 0$. Note that the functions $f_n(t)$ can be computed from the data $v(x,1,t)$ over the same time range.

Substituting (3.33) for $v(x,1,t)$ (and knowing that $\int_0^L \cos(\lambda_j x)\cos(\lambda_n x)dx = 0$ unless $j = n$) gives us

$$f_n(t) = \sum_{m=0}^{\infty}(-1)^m\frac{a_{nm}}{\mu_{nm}}(1-e^{-\mu_{nm}t}) \tag{3.35}$$

for all $n \geq 1$ while

$$f_0(t) = a_{00}t + \sum_{m=1}^{\infty}(-1)^m \frac{a_{0m}}{\mu_{0m}}(1 - e^{-\mu_{0m}t}) \tag{3.36}$$

if $n = 0$. If we use (3.31) to replace a_{nm} in (3.35) we obtain

$$\begin{aligned} f_n(t) &= 2\sum_{m=0}^{\infty}\sum_{\substack{k=1\\k\neq n}}^{\infty}\frac{(-1)^m}{\mu_{nm}}(1-e^{-\mu_{nm}t})q_{nm}\frac{k^3 S_k(1+(-1)^{n+k+1}}{\pi(n^2-k^2)(k^2+m^2L^2)} \\ &= 2\sum_{\substack{k=1\\k\neq n}}^{\infty}\left(\sum_{m=0}^{\infty}\frac{(-1)^m q_{nm}(1-e^{-\mu_{nm}t})k^3(1+(-1)^{n+k+1})}{\pi\mu_{nm}(n^2-k^2)(k^2+m^2L^2)}\right)S_k \end{aligned} \tag{3.37}$$

In the case $n = 0$, using (3.32) and (3.36)

$$\begin{aligned} f_0(t) &= -\sum_{k=1}^{\infty}\left(\frac{2t(1+(-1)^{k+1}}{\pi k}\right)S_k \\ &+ \sum_{m=1}^{\infty}\sum_{k=1}^{\infty}\frac{2(-1)^m q_{0m}k^3(1+(-1)^{k+1})(1-e^{-\mu_{0m}t})}{\pi\mu_{0m}(-k^2)(k^2+m^2L^2)}S_k \\ f_0(t) &= -\sum_{k=1}^{\infty}\left(\frac{2t(1+(-1)^{k+1}}{\pi k}\right)S_k \\ &- \sum_{m=1}^{\infty}\sum_{k=1}^{\infty}\frac{2(-1)^m q_{0m}k(1+(-1)^{k+1})(1-e^{-\mu_{0m}t})}{\pi\mu_{0m}(k^2+m^2L^2)}S_k. \end{aligned} \tag{3.38}$$

Equations (3.37) and (3.38) can be summarized as

$$f_n(t) = \sum_{k=1}^{\infty} M_{nk}(t)S_k \tag{3.39}$$

where

$$\begin{aligned} M_{nk}(t) &= 2\sum_{m=0}^{\infty}\frac{(-1)^m q_{nm}(1-e^{-\mu_{nm}t})k^3(1+(-1)^{n+k+1})}{\pi\mu_{nm}(n^2-k^2)(k^2+m^2L^2)}, k\neq n, n\neq 0 \\ M_{0k}(t) &= -\frac{2t(1+(-1)^{k+1})}{\pi k} - \sum_{m=1}^{\infty}\frac{2(-1)^m q_{0m}k(1+(-1)^{k+1})(1-e^{-\mu_{0m}t})}{\pi\mu_{0m}(k^2+m^2L^2)}. \end{aligned}$$

We can express this as

$$\vec{f}(t) = \begin{bmatrix} f_0(t) \\ f_1(t) \\ \vdots \end{bmatrix} = \begin{bmatrix} M_{0,1}(t) & M_{0,2}(t) & \cdots \\ M_{1,1}(t) & M_{1,2}(t) & \\ \vdots & & \ddots \end{bmatrix}\begin{bmatrix} S_1 \\ S_2 \\ \vdots \end{bmatrix} = M(t)\vec{S}. \tag{3.40}$$

Fix N, and let us assume that $S_n = 0$ for all $n > N$. Then also disregarding $f_{n-1}(t)$ for $n > N$, this becomes an approximate transformation $\tilde{M}(t)$ from one finite-dimensional vector space to another. The vector-valued function $\vec{f}(t)$ can be computed, and so $\vec{S}$ can be computed from $M(t)\vec{S} = \vec{f}(t)$, a system of linear equations for the S_k. We can use whatever value for N is appropriate, and any number of times. The resulting system is likely to be over-determined, but can be solved in a least-squares sense. Using multiple time values help determine a better approximation of S_k when noise is added to the top surface thermal data $\bar{v}(x, 1, t)$.

3.4 Numerical Approximation and Examples

We used the same process for constructing a damaged rectangle (same dimensions) as in the electrical case. However instead of measuring voltage, we measured heat at 401 spots distributed uniformly across the top surface. We did this every .05 seconds for 5 seconds total giving us 101 time samples at each position. Figure 3.1 shows our approximation with $N = 128$. Similarly the dashed line is the actual damage profile with the solid line is our approximation.

Note that the differentiation in (2.20) limits us to obtaining $S(x)$ to within an additive constant. Thus we make the assumption that the damage is confined to within an interval of the boundary, such as $\left[\frac{L}{10}, \frac{9L}{10}\right]$, and that $S(x) = 0$ at the endpoints of this interval. Taking the average value of our image at these points allows us to shift it by an appropriate amount. Thus we obtain an image from the electrothermal data.

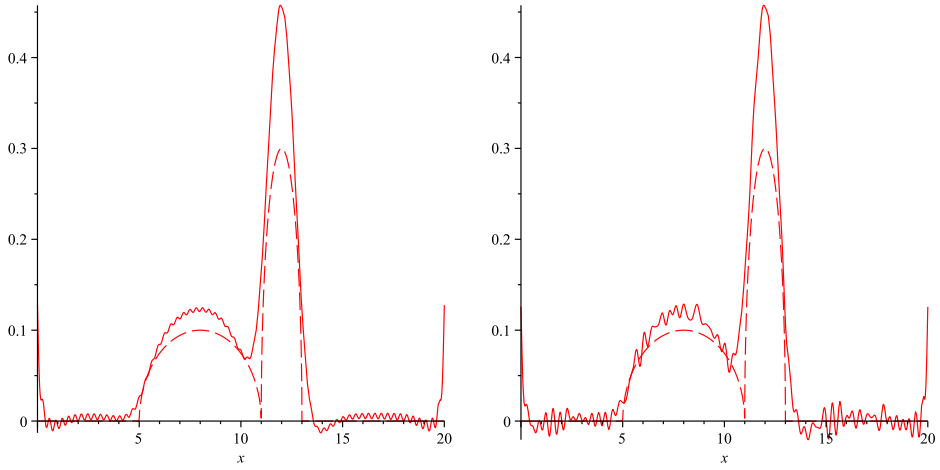

Figure 3.1: Approximation with no noise (left) and noise=.01 (right)

3.5 Summary

Much as in Chapter 2, the nonlinear map may be usefully approximated as a linear map, and this permits the reconstruction of the damage profile. This method shows less noise at high frequencies, and so can reproduce relatively fine scale features of the damage. It can be applied with a single image of temperature at a single time, but is improved by the addition of data from multiple times.

Chapter 4

Conclusion

Both electric and electrothermal methods allow images of an inaccessible boundary to be obtained. A careful analysis of the relative merits is yet to come. However, electrothermal imaging appears to be more powerful, as it does not suffer from the high-frequency instability of electrical imaging. Regularization, as used to control this instability, limits the resolution of electrical imaging. Electrothermal imaging also appears able to exploit an abundance of time-slices to reduce noise. This should be interpreted cautiously, however, as this advantage may depend on the type of noise. For instance, if noise is spatial (but constant in time), it is not expected that the inclusion of multiple time-slices will provide any benefit.

Much work remains to be done for the electrothermal imaging technique. For example, it is known that the electrical imaging problem has a unique solution $S(x)$ both for the linear approximation (this is Lemma 1) and for the fully nonlinear problem. The uniqueness question is open for both the linearized and fully nonlinear electrothermal problem, that is, given $v(x, 1, t)$, does there exist $S(x)$, unique up to an additive constant, which induces the temperature $v(x, 1, t)$? Initially it might appear that any finite subset of the Fourier coefficients could be fixed arbitrarily, and the remaining coefficients determined by taking a finite subset of the remaining matrix as before. If so, this allows us to construct multiple solutions. However, it is possible that all such alternate solutions fail to converge, leaving only a single unique solution in L^2. Either proving that this is so, or finding a counter-example, will be sufficient to determine the question of uniqueness.

The system (3.40) also needs much more analysis, to establish not only uniqueness but also stability. Such an analysis would also give insight into how one should choose that times at which the $f_n(t)$ are estimated, to maximize resolution and stability.

Acknowledgements

This work was supported, in part, by Rose-Hulman Institute of Technology and the National Science Foundation's Research for Undergraduates (REU) Sites Program Award DMS-1003924. Special thanks to Dr. Kurt Bryan, Professor of Mathematics at Rose-Hulman Institute of Technology, for his supervision and support.

Bibliography

[NS] N Stilwell, *Nondestructive Evaluation and Inverse Problems: The Electric Model*, U.S Air Force Academy senior thesis, Department of Mathematics, 2010-2011 academic year.

[KB] K Bryan, Personal Correspondence, July 10, 2011.